Deep Learning Framework using Sparse Diffusion MRI for Diagnosis of Frontotemporal Dementia

Abhishek Tiwari, Ananya Singhal, Saurabh J. Shigwan, Rajeev Kumar Singh
Department of Computer Science and Engineering,
Shiv Nadar Institution of Eminence, Delhi NCR, India
{at326,as146,saurabh.shigwan,rajeev.kumar}@snu.edu.in
for the Frontotemporal Lobar Degeneration Neuroimaging Initiative*

Abstract

Frontotemporal dementia (FTD) is a devastating neurodegenerative disorder that primarily affects the frontal and temporal lobes of the brain, leading to cognitive decline and behavioral changes. Early and accurate diagnosis of FTD is crucial for initiating timely interventions and providing appropriate care to patients. In the opinion of the experts , about 12-22 persons out of the population of 100,000 persons experience FTD. That means between 1.2 million and 1.8 million people have it worldwide. This research paper proposes a novel deep learning framework that utilizes sparse diffusion measures extracted from neuroimaging data to aid in the early diagnosis of Frontotemporal Dementia. The proposed model leverages the power of deep learning techniques to automatically learn relevant features from the data and effectively distinguish between healthy individuals and those with FTD. The experimental results demonstrate the promising potential of the proposed approach in improving FTD diagnosis and paving the way for future research in this area.

*Data used in preparation of this article were obtained from the Frontotemporal Lobar Degeneration Neuroimaging Initiative (FTLDNI) database. The investigators at NIFD/FTLDNI contributed to the design and implementation of FTLDNI and/or provided data, but did not participate in analysis or writing of this report (unless otherwise listed). The FTLDNI investigators can be found at:NIFD/FTLDNI investigators

1. Introduction

Frontotemporal Dementia(FTD) is a neurodegenerative disorder, impacting millions of people globally [12, 19]. The current clinical diagnosis involves time-consuming Diffusion Weighted Imaging (DWI), requiring at least 40 diffusion directions and leading to scanning durations exceeding three hours [18, 21]. Early and precise diagnosis is crucial for effective treatment and management [8, 16]. Diffusion tensor imaging (DTI) is a powerful neuroimaging technique that provides valuable information on the brain's white matter, often affected in FTD patients [5, 17, 26]. However, traditional linear methods for DTI processing require numerous diffusion directions, posing challenges for patients and diagnostic labs. Recent advances in deep learning [1, 2, 3, 15, 23, 24] show promise in accelerating DTI processing and improving quantitative measures for FTD diagnosis. Attention-based deep learning, like Transformer-DTI [10], focuses on relevant brain regions, enabling efficient processing with fewer diffusion directions. However, scalability becomes a concern with more diffusion directions due to increased trainable parameters, longer training times, and higher memory requirements.

To address this, we propose a novel Swin-Transformer attention-based deep learning model. The Swin Transformer's hierarchical structure efficiently processes input feature maps by dividing them into non-overlapping patches, reducing computational costs and parameter count. We aim to diagnose early FTD incidence accurately by extracting quantitative measures such as Fractional Anisotropy (FA), Axial Diffusivity (AD), and Mean Diffusivity(MD) using our proposed model on the frontotemporal lobar degeneration neuroimaging initiative (NIFD) dataset. We compare its performance with traditional linear methods and Transformer-DTI for different diffusion directions.

The main contributions of this article are as follows:

- Efficiently learning spatial correlation in neighboring voxels to improve robustness of estimations of DTI parameters.
- Introducing a Framework for DTI Parameter Estimation Utilizing Sparse Measurements while Maintaining Comparable Estimate Quality to Dense Measurements.
- Demonstrating the capability of DTI parameter esti-

mates of proposed model, to produce distinguishing features for healthy and FTD patients.

The paper proceeds with a detailed description of our proposed method and architecture in Section 2, followed by experimental results and analysis in Section 3. We conclude with a summary of our findings and future research directions in Section 4.

2. METHOD

A DWI image is a four-dimensional representation, with the first three dimensions denoting spatial measurements and the fourth dimension indicating water diffusivity across various diffusion directions. DTI, a specific type of DWI, captures diffusion anisotropy by utilizing a Gaussian model that considers diffusivity as a function of orientation [4, 13]. This orientation function is characterized by a 3×3 symmetric matrix D, represented as Equation 1.

$$D = \begin{bmatrix} D_{xx} & D_{xy} & D_{xz} \\ D_{yx} & D_{yy} & D_{yz} \\ D_{zx} & D_{zy} & D_{zz} \end{bmatrix} \tag{1}$$

The tensor D represents the magnitude of diffusivity on the surface of an ellipsoid, with its eigenvectors and eigenvalues corresponding to the directions and lengths of the ellipsoid's axes, respectively. The diffusion signal within each 3D voxel is a vector $\mathbf{s} = [s_1, s_2, ..., s_N]$, and according to the DTI formulation [13] shown in Equation 2, we aim to extract the diffusion tensor D from the signal $\mathbf{s}$.

$$s_i = s_0 e^{(-b_{xx}D_{xx} - b_{yy}D_{yy} - b_{zz}D_{zz} - 2b_{xy}D_{xy} - 2b_{xz}D_{xz} - 2b_{yz}D_{yz})} \tag{2}$$

Here, b_{jk}, for $j, k \in \{x, y, z\}$, represents function of diffusion directions $\mathbf{g} = \{g_i\}_{i=1}^{N}$, where each $g_i = [g_{ix}, g_{iy}, g_{iz}]$ is a unit direction vector. Additionally, s_0 represents zero diffusion signal. By simplifying the b-matrix as given in [13], we obtain the equation $s_i/s_0 = e^{-bg_i^T D g_i}$, which provides the best accuracy of the diffusion coefficient D. The apparent diffusion coefficient K_i with respect to each g_i can be calculated as $K_i = g_i^T D g_i = (-1/b)\ln(s_i/s_0)$.

The design matrix $\alpha = [\alpha_1, ..., \alpha_N]^T$ represents the linear mapping between the diffusion tensor D and the apparent diffusion coefficient estimates $K = [K_1, ..., K_N]^T$ using $K = \alpha \bar{D}$, where $\bar{D} = [D_{xx}, D_{yy}, D_{zz}, D_{xy}, D_{xz}, D_{yz}]^T$ and $\alpha_i = [g_{ix}^2, g_{iy}^2, g_{iz}^2, 2g_{ix}g_{iy}, 2g_{ix}g_{iz}, 2g_{iy}g_{iz}]^T$. The traditional linear least squares fitting (LLS) method [11] uses $\bar{D} = (\alpha^T\alpha)^{-1}\alpha^T K$, which is susceptible to noise and sparse measurements.

For sparse measurements, instead of using the linear model, we propose solving for D directly using Equation 2 as an inverse map $\bar{D} = F(\mathbf{X}, \mathbf{g})$, where the input $\mathbf{X} = [s_1/s_0, ..., s_N/s_0]$ per voxel. We have formulated F using a Swin-transformer based neural network [14]. Our modeling framework is a more generic approach, where a single

Algorithm 1 Preprocessing the data for the proposed model

The preprocessing algorithm for DWI images from the NIFD dataset involves creating three preprocessed training datasets: $NIFD-41$, $NIFD-21$, and $NIFD-5$.

Step 1: Utilize the DTI model fitting procedure available in the DIPY Python package[9] to process each individual DWI image separately. This process yields six distinct diffusion components, namely D_{xx}, D_{xy}, D_{yy}, D_{xz}, D_{yz}, which collectively constitute the diffusion tensor.
Step 2: Choose $20,000$ voxels from each DWI image by evaluating their fractional anisotropy (FA) score. Voxel selection should disregard zero values and maintain a uniform distribution across the interval $(0, 1)$.
Step 3: Collect a dataset comprising $20,000$ pairs of (input, ground-truth), with each pair containing a $5 \times 5 \times 5$ voxel patch as the input. This patch is characterized by 41 diffusion directions per voxel. The corresponding ground-truth component encompasses a $5 \times 5 \times 5$ voxel patch, where each voxel is associated with a 6×1 vector representing the six diffusion components of the diffusion tensor.
Step 4: Create a matrix of dimensions 125×41 for each input voxel by combining the diffusion signals from the adjacent $5 \times 5 \times 5$ patch.
Step 5: Concatenate the diffusion directions (3×41) with the diffusion signal to yield a matrix of dimensions 128×41 for each input voxel.
Step 6: Perform zero-padding on the input of every tuple, resulting in a 128×100 matrix, while the corresponding ground truth is depicted as a 125×6 matrix. The resultant collection of training data is referred to as $NIFD-41$.
Step 7: Utilizing the DIPY package, apply Qball-based interpolation [25, 9] to the 41-directional input from the $NIFD-41$ dataset. This process will yield diffusion signals with 41, 21, and 5 directions, respectively.
Step 8: Concatenate the diffusion directions and diffusion signals within each tuple to generate input vectors of dimensions 125×41, 125×21, and 125×5, as well as a ground truth matrix of size 125×6.
Step 9: Apply zero-padding to the input of every tuple, resulting in the formation of a matrix sized 128×100.
Step 10: The generated training datasets are denoted as $NIFD-41$, $NIFD-21$, and $NIFD-5$, corresponding to the specific diffusion directions of 41, 21, and 5 respectively.

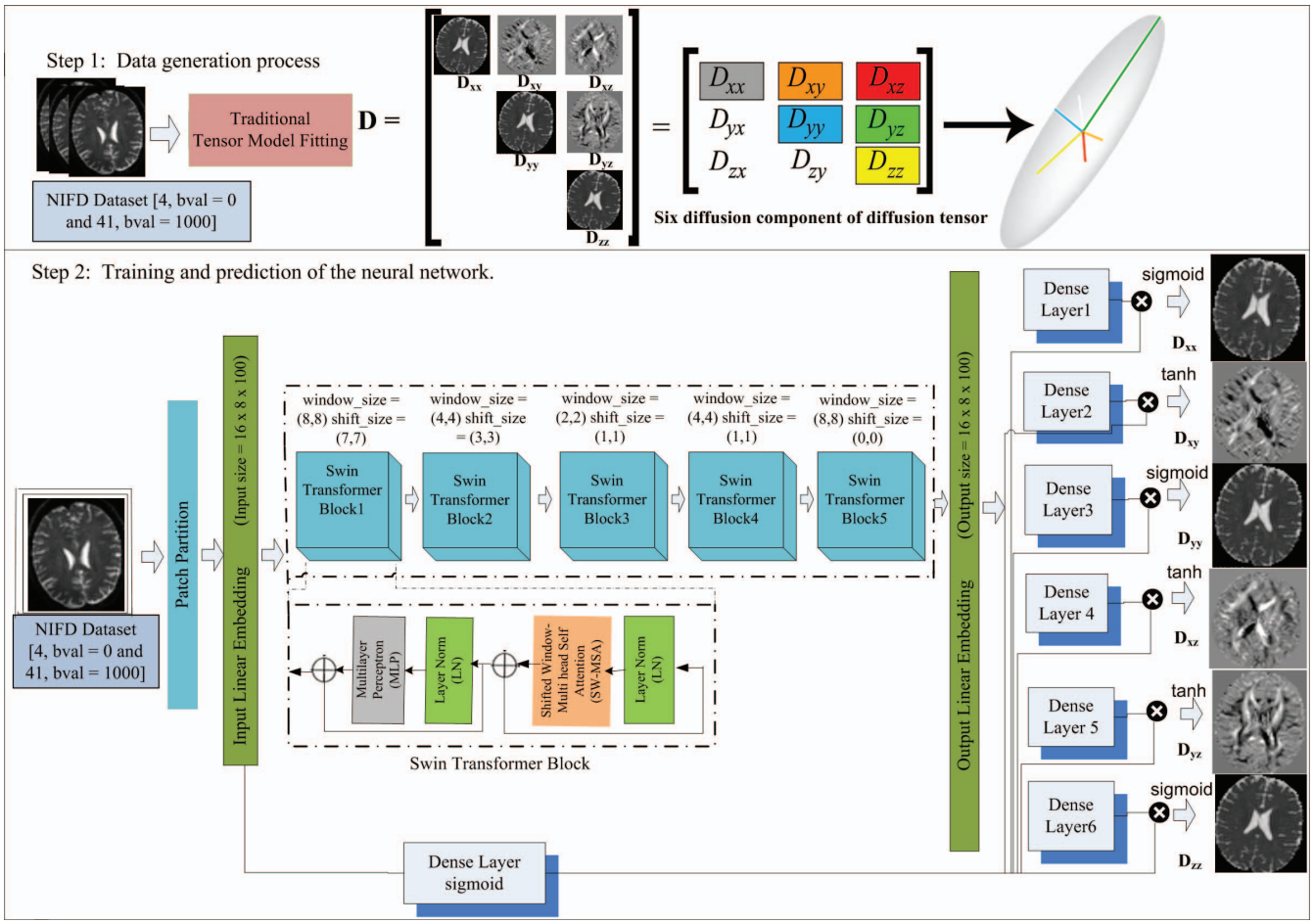

Figure 1. The proposed model architecture for training and prediction of the neural network.

Table 1. The number of pixels with p-values outside Confidence Intervals (95% and 99%) for t-statistics (tstat1 and tstat2) in the Proposed Model, LLS fitting, and Transformer-DTI, with tstat1 hypothesis comparing Healthy CN > FTD patient and tstat2 hypothesis comparing Healthy CN < FTD patient.

P-Value	Ground Truth	Proposed Model		LLS fitting		Transformer-DTI	
		5 Diff.	21 Diff.	5 Diff.	21 Diff.	5 Diff.	21 Diff.
tstat1, 95 C.I.	15870	9924	14471	13844	18262	9481	17820
tstat2, 95 C.I.	4294	7527	5719	5391	4351	12162	4517
tstat1, 99 C.I.	3591	2418	3564	3585	4836	2510	4866
tstat2, 99 C.I.	837	1702	1450	1061	913	3818	1181

model can efficiently learn from diffusion signals with different numbers of diffusion directions (e.g., $41, 21, 5$).

In practical applications, multiple attention heads are commonly used to learn diverse representations of the input. The Transformer-DTI [10] model employed multi-head self-attention to estimate diffusion tensor imaging parameters using only six diffusion-weighted images.

In our proposed model, we introduce a modified version of window self-attention to enhance non-linearity and decrease the number of parameters. This window self-attention mechanism offers several advantages over traditional self-attention mechanisms, making it a crucial component. Instead of embedding the diffusion directions implicitly using learned weights, we concatenate the direction vector as part of the input signal. This enhancement improves the model's non-linearity and enables it to capture more intricate relationships within the input data. Traditionally, self-attention applies distinct triplets of (query, key, value) to each position in the input. However, in our proposed model, we employ window self-attention, where the

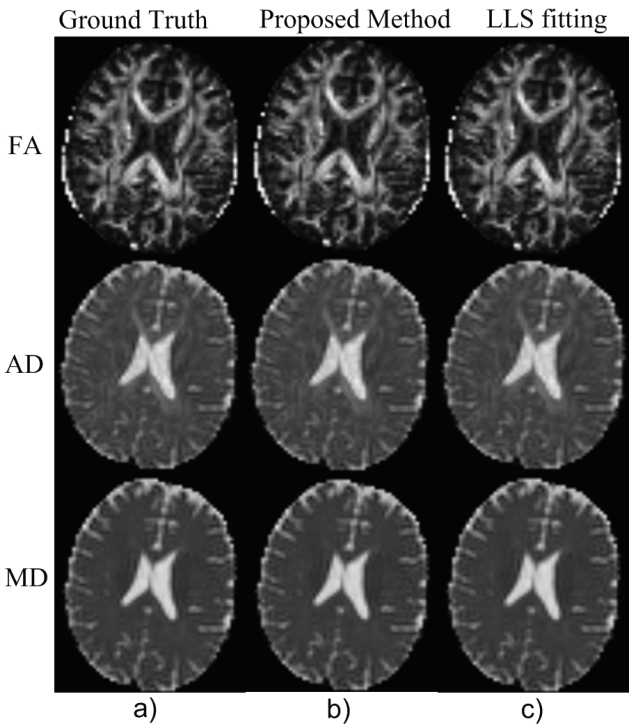

Figure 2. Comparison of 41 diffusion directions: Ground truth vs. Proposed method vs. LLS fitting [11]

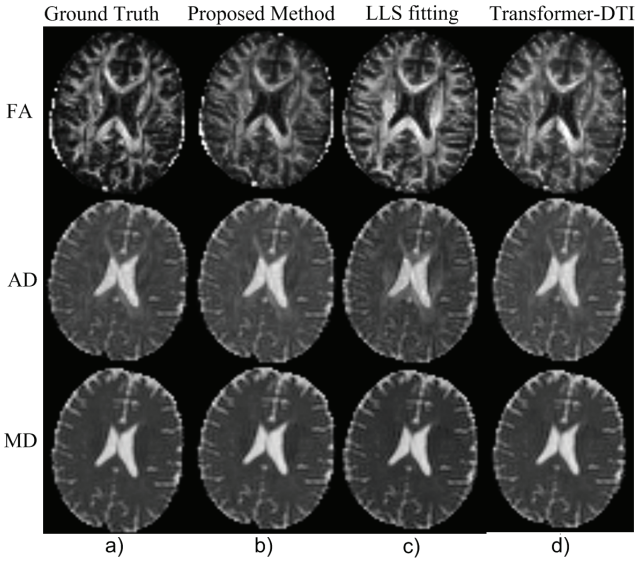

Figure 3. Comparison of 21 diffusion directions: Ground truth vs. Proposed method vs. LLS fitting [11] and Transformer-DTI [10]

same triplets are applied to all windows within the same patch. This patch-based method divides the input matrix into patches and independently applies spatial relative attention to each patch, reducing the computational burden of spatial relative attention and allowing for the modeling of long-range spatial relationships in large images.

In our proposed model based on the Swin Transformer

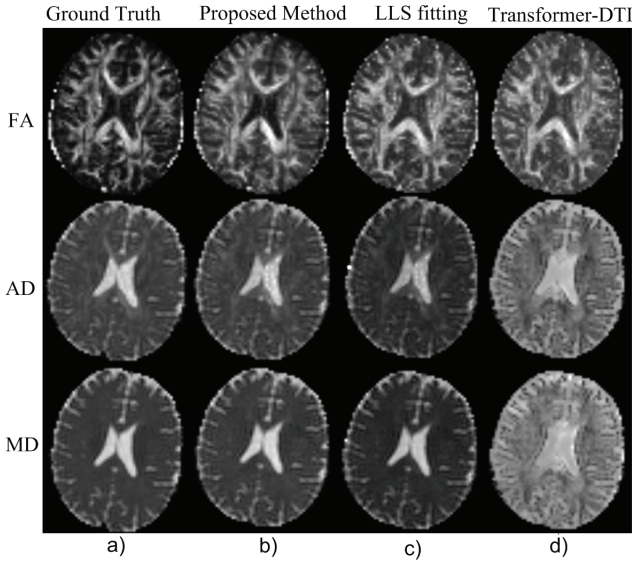

Figure 4. Comparison of 5 diffusion directions: Ground truth vs. Proposed method vs. LLS fitting [11] and Transformer-DTI [10]

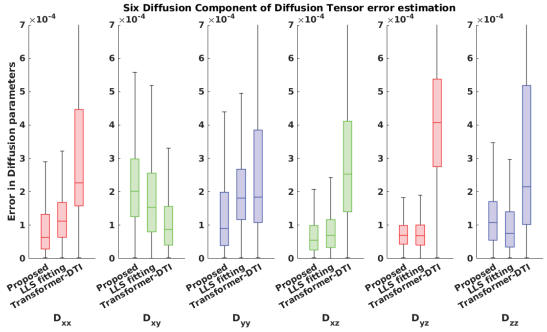

Figure 5. Six diffusion components of diffusion tensor for 5 diffusion directions

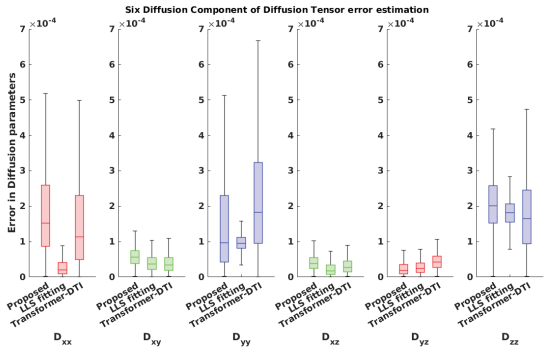

Figure 6. Six diffusion components of diffusion tensor for 21 diffusion directions

architecture, neighboring windows are strategically shifted using a designated stride, resulting in overlapping regions between adjacent windows. This strategic overlap serves to facilitate inter-token attention, enabling tokens to establish connections with one another even when they belong to dif-

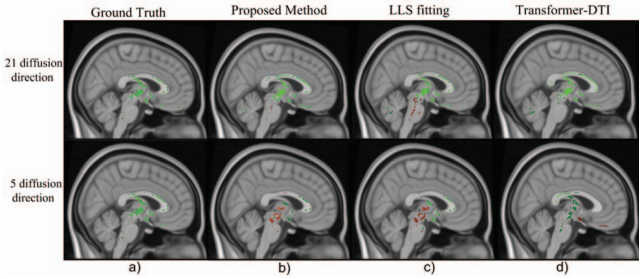

Figure 7. Axial brain slice representing the Cingulum region, highlighted with p-value of two sample t-test(df=8). Green color: hypothesis testing tstat1 - Healthy CN $>$ FTD patient, Red color: hypothesis testing tstat2 - Healthy CN $<$ FTD patient.

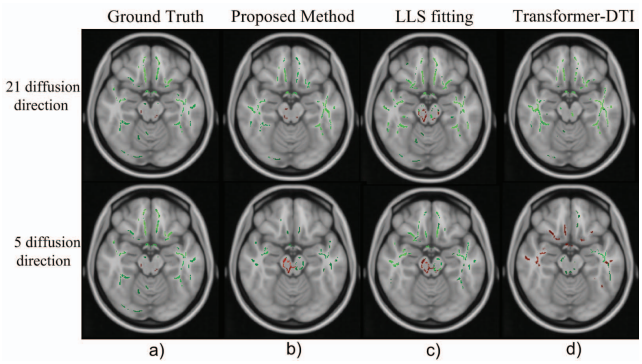

Figure 8. Coronal brain slice representing the Uncinate fasciculus region, highlighted with p-value of two sample t-test(df=8). Green color: hypothesis testing tstat1 - Healthy CN $>$ FTD patient, Red color: hypothesis testing tstat2 - Healthy CN $<$ FTD patient.

ferent windows. This dynamic interaction between tokens introduces an expanded array of opportunities for mutual influence, thereby nurturing the development of more intricate and enriched representations.

As a component of our proposed model, we have incorporated a novel activation function that is based on element-wise multiplication. Specifically, in our system, the values of D_{xx}, D_{yy}, D_{zz} are restricted to a range between 0 and 1, while the values of D_{xy}, D_{yz}, D_{xz} are limited to a range between -1 and 1. To handle these distinct ranges, we utilized the $sigmoid$ activation function for the former set and the $tanh$ activation function for the latter set. Additionally, the magnitude of the outputs $\bar{D}$ is a nonlinear function of the magnitude of the DWI signals. To incorporate this knowledge, we multiplied the final outputs by the output of a Sigmoid-activated dense layer on the DWI signal. This innovative approach enabled us to modulate the output magnitude of the estimates, which in turn reduced the training time and improved the overall accuracy of our proposed framework.

2.1. Data Preprocessing and Model Training

We developed an algorithm to preprocess diffusion-weighted imaging (DWI) images from the NIFD dataset, resulting in three preprocessed training datasets: $NIFD-41$, $NIFD-21$, and $NIFD-5$. The preprocessing algorithm is outlined in Algorithm 1 [9, 25].

Our neural network was trained on a dataset consisting of 20,000 tuples per image obtained from three different datasets: $NIFD-41$, $NIFD-21$, and $NIFD-5$ [9, 25]. These tuples were derived from a subset of 24 diffusion-weighted imaging (DWI) images, preprocessed using *Algorithm 1*. The architecture of our neural network is illustrated in Figure 1, where we employ a Swin-transformer block known for its ability to capture correlations within input signals [14]. In our case, the input signals consist of diffusion signals along with diffusion directions, and our model considers the diffusion signals within a neighboring $5 \times 5 \times 5$ patch along with the current voxel diffusion signal.

3. Results and Discussions

In our experiments, we employed 54 DWI images from the NIFD dataset, comprising 27 from the Cognitively Normal (CN) group and 27 from the FTD patient group. To train our model, we used 12 CN and 12 FTD patient images, with 3 from each group used for validation. The remaining 12 CN and 12 FTD patient images were reserved for testing. We considered the output of LLS fitting over NIFD-41 as ground truth for our experiments. To evaluate the performance of our proposed method, we compared its results with LLS fitting and Transformer-DTI. Figure 2 illustrates the comparisons of ground truth, proposed method, and LLS fitting for 41 diffusion directions. The results demonstrate that the proposed method is comparable to LLS fitting, accurately estimating diffusion tensor parameters. Figure 3 presents the diffusion measures for 21 diffusion directional signals, while Figure 4 shows the results for 5 diffusion directional signals using the proposed method, LLS fitting, and Transformer-DTI. Our proposed method shows comparable performance to LLS fitting [11] for 21 diffusion directions (Figures 3 and 6), and outperforms Transformer-DTI [10]. For 5 diffusion directions, our model surpasses both LLS fitting and Transformer-DTI (Figures 4 and 5), demonstrating its effectiveness in accurately estimating diffusion measures, especially with fewer diffusion directions. Error plots of six diffusion components $\bar{D}$ for 5 and 21 diffusion directional signals are presented in Figures 5 and 6, respectively. Furthermore, the study employed a t-test analysis using the tract-based spatial statistics (TBSS) pipeline [22] to assess the statistical significance of our results. The analysis compared two groups, Healthy CN and FTD patients, based on fractional anisotropy (FA) metrics. FA images were registered to the FMRIB-58 template in the MNI

space using FNIRT from FSL [20]. The white matter skeleton was derived from a mean FA image with an FA threshold of 0.2, enabling a reliable statistical interpretation of the data. Figures 7 and 8 show axial and coronal brain slices highlighting the Cingulum and Uncinate fasciculus regions with p-values obtained from two sample t-tests. The results reveal significant associations between FTD patients and the Cingulum and Uncinate fasciculus regions, consistent with previous studies [6, 7]. Our proposed framework demonstrates a similar relationship with sparse data, reducing scanning time significantly. These white matter tracts play a crucial role in various cognitive processes, and alterations in their microstructural integrity may be linked to the onset of FTD. Table 1 compares the number of pixels with p-values outside confidence intervals for different diffusion directions (5 Diff. and 21 Diff.) at 95% and 99% confidence intervals. The results demonstrate that our proposed method maintains an equal number of pixels with significant differences compared to the ground truth, whereas the LLS fitting and Transformer-DTI methods show greater deviations from the ground truth.

4. CONCLUSION

In conclusion, the potential of the proposed Swin-Transformer-based deep learning framework, integrating sparse diffusion measures, as a promising approach for early diagnosis of FTD patients. By incorporating sparse diffusion measures, our framework effectively captures the underlying structural connectivity of the brain, a critical feature in FTD patients. Through this innovative approach, the Swin-Transformer-based deep learning model successfully learns the intricate relationships between brain connectivity patterns and disease status, facilitating accurate diagnosis of FTD patients at an early stage. The results of this study encourage further investigation of the framework's capabilities in large-scale clinical trials, offering the potential to contribute significantly to the field of neurodegenerative disorder diagnosis. Future research can also explore the framework's effectiveness in detecting FTD patients in diverse populations, potentially expanding its applications to a broader range of individuals. Our proposed Swin-Transformer-based deep learning framework presents a promising avenue for enhancing early detection and diagnosis of FTD patients, which may lead to more effective interventions and improved patient care.

Declarations

Conflict of interest The authors declare that they have no conflict of interest.

Data availability The data utilized in this article were acquired from the Frontotemporal Lobar Degeneration Neuroimaging Initiative (FTLDNI) database. All experimental results are accessible upon genuine request.

References

[1] Karim Aderghal, Karim Afdel, Jenny Benois-Pineau, and Gwénaëlle Catheline. Improving alzheimer's stage categorization with convolutional neural network using transfer learning and different magnetic resonance imaging modalities. *Heliyon*, 6(12), 2020.

[2] Santiago Aja-Fernández, Carmen Martín-Martín, Álvaro Planchuelo-Gómez, Abrar Faiyaz, Md Nasir Uddin, Giovanni Schifitto, Abhishek Tiwari, Saurabh J Shigwan, Rajeev Kumar Singh, Tianshu Zheng, et al. Validation of deep learning techniques for quality augmentation in diffusion mri for clinical studies. *NeuroImage: Clinical*, page 103483, 2023.

[3] Sukrit Arora, Michael Lustig, and Stella Yu. Deep learning applications in computational mri: A thesis in two parts. 2021.

[4] Peter J Basser, James Mattiello, and Denis LeBihan. Mr diffusion tensor spectroscopy and imaging. *Biophysical journal*, 66(1):259–267, 1994.

[5] Ayşe Demirhan, Talia M Nir, Artemis Zavaliangos-Petropulu, Clifford R Jack, Michael W Weiner, Matt A Bernstein, Paul M Thompson, and Neda Jahanshad. Feature selection improves the accuracy of classifying alzheimer disease using diffusion tensor images. pages 126–130, 2015.

[6] John S Duncan. Imaging in the surgical treatment of epilepsy. *Nature Reviews Neurology*, 6(10):537–550, 2010.

[7] Negar Fani, Tricia Z King, Emily Reiser, Elisabeth B Binder, Tanja Jovanovic, Bekh Bradley, and Kerry J Ressler. Fkbp5 genotype and structural integrity of the posterior cingulum. *Neuropsychopharmacology*, 39(5):1206–1213, 2014.

[8] Shuangshuang Gao and Dimas Lima. A review of the application of deep learning in the detection of alzheimer's disease. *International Journal of Cognitive Computing in Engineering*, 3:1–8, 2022.

[9] Eleftherios Garyfallidis, Matthew Brett, Bagrat Amirbekian, Ariel Rokem, Stefan Van Der Walt, Maxime Descoteaux, Ian Nimmo-Smith, and Dipy Contributors. Dipy, a library for the analysis of diffusion mri data. *Frontiers in neuroinformatics*, 8:8, 2014.

[10] Davood Karimi and Ali Gholipour. Diffusion tensor estimation with transformer neural networks. *Artificial Intelligence in Medicine*, page 102330, 2022.

[11] Cheng Guan Koay, Lin-Ching Chang, John D Carew, Carlo Pierpaoli, and Peter J Basser. A unifying theoretical and algorithmic framework for least squares methods of estimation in diffusion tensor imaging. *Journal of magnetic resonance*, 182(1):115–125, 2006.

[12] Shayan Kolahkaj et al. A connectome-based deep learning approach for early mci and mci detection using structural brain networks. *Neuroscience Informatics*, page 100118, 2023.

[13] Denis Le Bihan, Jean-François Mangin, Cyril Poupon, Chris A Clark, Sabina Pappata, Nicolas Molko, and Hughes

Chabriat. Diffusion tensor imaging: concepts and applications. *Journal of Magnetic Resonance Imaging: An Official Journal of the International Society for Magnetic Resonance in Medicine*, 13(4):534–546, 2001.

[14] Ze Liu, Yutong Lin, Yue Cao, Han Hu, Yixuan Wei, Zheng Zhang, Stephen Lin, and Baining Guo. Swin transformer: Hierarchical vision transformer using shifted windows. pages 10012–10022, 2021.

[15] Zhenbing Liu, Haoxiang Lu, Xipeng Pan, Mingchang Xu, Rushi Lan, and Xiaonan Luo. Diagnosis of alzheimer's disease via an attention-based multi-scale convolutional neural network. *Knowledge-Based Systems*, 238:107942, 2022.

[16] Eman N Marzban, Ayman M Eldeib, Inas A Yassine, Yasser M Kadah, and Alzheimer's Disease Neurodegenerative Initiative. Alzheimer's disease diagnosis from diffusion tensor images using convolutional neural networks. *PloS one*, 15(3):e0230409, 2020.

[17] Talia M Nir, Neda Jahanshad, Julio E Villalon-Reina, Arthur W Toga, Clifford R Jack, Michael W Weiner, Paul M Thompson, Alzheimer's Disease Neuroimaging Initiative (ADNI, et al. Effectiveness of regional dti measures in distinguishing alzheimer's disease, mci, and normal aging. *NeuroImage: clinical*, 3:180–195, 2013.

[18] Shangran Qiu, Matthew I Miller, Prajakta S Joshi, Joyce C Lee, Chonghua Xue, Yunruo Ni, Yuwei Wang, Ileana De Anda-Duran, Phillip H Hwang, Justin A Cramer, et al. Multimodal deep learning for alzheimer's disease dementia assessment. *Nature communications*, 13(1):3404, 2022.

[19] Yida Qu, Pan Wang, Bing Liu, Chengyuan Song, Dawei Wang, Hongwei Yang, Zengqiang Zhang, Pindong Chen, Xiaopeng Kang, Kai Du, et al. Ai4ad: artificial intelligence analysis for alzheimer's disease classification based on a multisite dti database. *Brain Disorders*, 1:100005, 2021.

[20] Daniel Rueckert, Luke I Sonoda, Carmel Hayes, Derek LG Hill, Martin O Leach, and David J Hawkes. Nonrigid registration using free-form deformations: application to breast mr images. *IEEE transactions on medical imaging*, 18(8):712–721, 1999.

[21] Benoit Scherrer and Simon K Warfield. Parametric representation of multiple white matter fascicles from cube and sphere diffusion mri. *PLoS one*, 7(11):e48232, 2012.

[22] Stephen M Smith, Mark Jenkinson, Heidi Johansen-Berg, Daniel Rueckert, Thomas E Nichols, Clare E Mackay, Kate E Watkins, Olga Ciccarelli, M Zaheer Cader, Paul M Matthews, et al. Tract-based spatial statistics: voxelwise analysis of multi-subject diffusion data. *Neuroimage*, 31(4):1487–1505, 2006.

[23] M Tanveer, MA Ganaie, Iman Beheshti, Tripti Goel, Nehal Ahmad, Kuan-Ting Lai, Kaizhu Huang, Yu-Dong Zhang, Javier Del Ser, and Chin-Teng Lin. Deep learning for brain age estimation: A systematic review. *Information Fusion*, 2023.

[24] Abhishek Tiwari and Rajeev Kumar Singh. Performance, trust, or both? covid-19 diagnosis and prognosis using deep ensemble transfer learning on x-ray images. pages 1–9, 2022.

[25] David S Tuch. Q-ball imaging. *Magnetic Resonance in Medicine: An Official Journal of the International Society for Magnetic Resonance in Medicine*, 52(6):1358–1372, 2004.

[26] Liang Zhan, Matt A Bernstein, B Borowski, Clifford R Jack, and Paul M Thompson. Evaluation of diffusion imaging protocols for the alzheimer's disease neuroimaging initiative. pages 710–713, 2014.